JMolMed CrossMark

ORIGINAL ARTICLE

Primary melanoma tumor inhibits metastasis through alterations in systemic hemostasis

Jennifer M. Kirstein[1,2] · M. Nicole Hague[1] · Patricia M. McGowan[1] · Alan B. Tuck[1,3,4] ·
Ann F. Chambers[1,2,3,4]

Abstract Progression from a primary tumor to distant metastases requires extensive interactions between tumor cells and their microenvironment. The primary tumor is not only the source of metastatic cells but also can also modulate host responses to these cells, leading to an enhancement or inhibition of metastasis. Tumor-mediated stimulation of bone marrow can result in pre-metastatic niche formation and increased metastasis. However, a primary tumor can also inhibit metastasis through concomitant tumor resistance—inhibition of metastatic growth by existing tumor mass. Here, we report that the presence of a B16F10 primary tumor significantly restricted numbers and sizes of experimental lung metastases through reduction of circulating platelets and reduced formation of metastatic tumor cell-associated thrombi. Tumor-bearing mice displayed splenomegaly, correlated with primary tumor size and platelet count. Reduction in platelet numbers in tumor-bearing animals was responsible for metastatic inhibition, as restoration of platelet numbers using isolated platelets reestablished both tumor cell-associated thrombus formation and experimental metastasis. Consumption of platelets due to a B16F10 primary tumor is a form of concomitant tumor

resistance and demonstrates the systemic impact of a growing tumor. Understanding the interplay between primary tumors and metastases is essential, as clarification of concomitant tumor resistance mechanisms may allow inhibition of metastatic growth following tumor resection.

Key messages
- Mice with a primary B16F10 tumor had reduced metastasis vs. mice without a primary tumor.
- Tumor-bearing mice had splenomegaly and fewer platelets and tumor-associated thrombi.
- Restoring platelets restored tumor-associated thrombi and increased metastasis.
- This work shows the impact that a primary tumor can have on systemic metastasis.
- Understanding these interactions may lead to improved ways to inhibit metastasis.

✉ Ann F. Chambers
ann.chambers@Lhsc.on.ca

1 London Regional Cancer Program, London Health Sciences Centre, 790 Commissioners Road East, London, ON N6A 4L6, Canada

2 Department of Medical Biophysics, University of Western Ontario, London, ON, Canada

3 Department of Pathology and Laboratory Medicine, University of Western Ontario, London, ON, Canada

4 Department of Oncology, University of Western Ontario, London, ON, Canada

Introduction

The evolution of metastatic disease from a primary tumor occurs though a series of essential steps—tumor cell invasion and intravasation, arrest in a distant capillary bed, extravasation and growth initiation in the secondary organ, and sustained growth with recruitment of a new vasculature [1]. Survival of metastatic cells during each of these steps depends on complex interactions with and evasion of host responses to both the primary tumor and metastatic cells [2, 3]. The potential for a primary tumor to inhibit development of distant metastases has long been acknowledged, with clinical evidence of massive metastatic outgrowth following removal of

multiple primary tumor types [4, 5]. The mechanism behind this process of "concomitant tumor resistance," the ability of a primary tumor to restrict the development of a second tumor, has not been resolved [6–8]. Better understanding of concomitant tumor resistance might lead to novel approaches to inhibit metastasis through supplementation or depletion of factors to mimic the presence of a primary tumor, and thereby continue secondary tumor growth restriction after primary tumor resection.

Three hypotheses have been proposed to explain the protection from metastatic growth by a primary tumor [9]: concomitant immunity, whereby a primary tumor may prime the host immune system and enhance clearance of metastatic cells; production of inhibitory factors (anti-mitogenic or anti-angiogenic) from the primary tumor which prevent growth of the secondary tumors; and athrepsia, the depletion of required systemic factors by the primary tumor thereby preventing metastatic establishment. Investigation of concomitant tumor resistance led to the discovery of anti-angiogenic factors produced by a primary tumor that are capable of preventing angiogenesis in secondary tumors [10–13]. Concomitant immunity has been found to occur only in highly immunogenic tumor types, such as those arising following chemical insult, and only while those tumors remained small (<500 mm^3) [14], unless animals were depleted of specific regulatory T cells [15]. The concept of athrepsia as it applies to metastatic growth has not been well investigated to date [7, 9].

It is well established that coagulation factors are essential to successful metastasis formation [16], especially for B16 murine melanoma cell lines [17–19]. Our group and others have shown that elimination of individual coagulation factors restricts pulmonary metastasis formation [17, 20–23], in part by allowing increased NK immune cell killing of tumor cells [19, 24, 25]. Stabilization of cell surface thrombi using the serine protease inhibitor aprotinin increased metastasis formation due to sustained interaction between thrombi and metastatic B16F10 cells [17]. B16F10 cells express tissue factor (TF) and are individually capable of activating the coagulation cascade [26]. Thus, it was hypothesized that cells within a B16F10 primary tumor may stimulate thrombus formation and may deplete systemic coagulation factors such as platelets. Platelets have long been hypothesized to support cancer progression and have been linked to increasing formation of metastases through increasing many important facets of metastasis, including sustained cell arrest and survival in the vasculature, extravasation, and proliferation in secondary tissues [19, 27–29]. Given that tumor cell-associated thrombi are essential for successful metastatic progression, we hypothesized that the presence of a B16F10 primary tumor in a mouse model would therefore restrict lung metastasis.

Here, we analyzed the effect of a B16F10 primary tumor on metastasis formation. We found a significant inhibition of lung metastasis formation following a secondary intravenous injection of B16F10-LacZ cells in primary tumor-bearing mice. This decrease was due to reduced thrombus formation at the metastatic site (lung) caused by a significant reduction in circulating platelet numbers. Re-constitution of platelet counts in tumor-bearing mice using isolated murine platelets restored cell surface thrombi and led to equivalent metastasis formation in tumor-bearing and tumor-naïve mice.

Material and methods

Cell culture

B16F10-LacZ [17] and B16F10 murine melanoma cells (American Type Culture Collection, Manassas, VA, USA) were maintained in α-minimal essential media (Invitrogen, Burlington, Canada), supplemented with 10 % fetal bovine serum (Sigma, Mississauga, Canada), and 1 mg/ml hygromycin (Invitrogen, B16F10-LacZ only). For injection into mice, cells were trypsinized from 70 to 80 % confluent plates and suspended in cold, sterile Hanks Balanced Salt Solution (HBSS, Invitrogen) to a final concentration of 5×10^6/mL.

Experimental metastasis model

Female C57Bl/6 mice (6–7 weeks old, Charles River) were lightly anesthetized with isoflurane and 100 μl of the B16F10 cell preparation (primary tumor group) or cell vehicle (HBSS, tumor-naïve group) was injected orthotopically into the dermis (i.d.) on the right hind flank. Tumor growth was evaluated by measurement with calipers in two perpendicular dimensions, and the tumor volume was estimated using the following formula volume = 0.52 (width)^2(length), for approximating the volume (mm^3) of an ellipsoid. Primary tumors were allowed to grow for 16 days, at which time B16F10-LacZ cells were trypsinized from 70 to 80 % confluent plates and suspended in cold, sterile HBSS. Unanesthetized tumor-bearing and tumor-naïve mice then received an intravenous (i.v.) injection of 5×10^5 cells in 100 μl HBSS via the lateral tail vein. Animals were sacrificed 6 days following i.v. injection and lung tissue was isolated, stained for β-galactosidase activity and the number of lung surface metastases quantified as previously described [17].

For platelet restoration studies, 100 μl of the platelet suspension (see "Platelet isolation and preparation" section) or vehicle was injected via the lateral tail vein 5 min prior to i.v. B16F10-LacZ cell injection. Animals were sacrificed 6 days following i.v. injection and lung tissue was isolated, stained for β-galactosidase activity, and the number of lung surface metastases quantified.

All mice were 7–8 weeks of age at the time of injection and were cared for in accordance to the Canadian Council on

Animal Care, under a protocol approved by the University of Western Ontario Council on Animal Care.

Quantification of lung metastases

To enable visualization of lung metastases, mice were euthanized 6 days following i.v. cell injection and whole lungs placed in phosphate buffer (0.1 M sodium phosphate monobasic, 0.1 M sodium phosphate dibasic, pH 7.3), on ice. Lungs were stained with X-gal (Bioshop, Burlington, Canada) solution as described [17] to visualize LacZ-expressing cells. The total number of surface-visible metastases was determined on intact lung lobes using a stereomicroscope. Area of individual lung metastases was determined using the Axiovert 200M microscope and Axiocam HRC camera utilizing Axiovision 4.6 software. Linear length and width of each metastasis was determined, and area of each was estimated by assuming an approximately elliptical shape and using the formula: $\pi \times length \times width / 4$.

Assessment of circulating platelet numbers

Sixteen days after hind flank injection of cell vehicle or B16F10 cells, tumor-naïve and B16F10 primary tumor-bearing mice were anesthetized with isoflurane and blood was drawn by cardiac puncture using a heparinized syringe and collected into purple top (EDTA) 2-mL tubes (BD Biosciences, Mississauga, Canada). The number of platelets was determined on a Coulter LH 780 Hematology analyzer. The normal platelet count seen in mice is $1000–1500 \times 10^3/\mu l$, but the number quantified on clinical hematology analyzers is frequently underestimated due to the smaller size of murine platelets [30]. To ensure that this did not skew our data, all quantifications were performed on the same machine. For platelet re-constitution studies, mice received an i.v. injection of platelets 5 min prior to cardiac puncture and blood collection as above to determine the number of platelets present when B16F10-LacZ cells would be delivered.

Platelet isolation and preparation

For platelet re-constitution experiments, blood was obtained from female C57Bl/6 retired breeders (30–35 g) under isoflurane anesthetic via cardiac puncture using citrated 3-mL syringes. Blood was collected into 2-mL Eppendorf tubes with citrate-dextrose solution (0.1 M trisodium citrate, 0.11 M dextrose, 71 mM citric acid monohydrate) at 1:9 citrate-dextrose/blood ratio. Platelets were isolated using a differential centrifugation protocol based on Musaji et al. [31]. Briefly, whole blood was centrifuged at $220g$ for 6 min at 4 °C and platelet-rich (PR) upper layer was collected. Cold, buffered saline glucose citrate (BSGC 8.6 mM Na_2HPO_4, 1.6 mM KH_2PO_4, 0.12 M NaCl, 0.9 mM EDTA, 13.6 mM NaCitrate,

11.1 mM D-Glucose, pH 7.3) was added to each tube to 1.75 mL and inverted to mix. PR upper layer was collected following another $220g$ spin for 6 min at 4 °C. This step was repeated once more. PR suspensions were pooled and centrifuged at $1613g$ for 15 min at 4 °C to pellet platelets. Supernatant was discarded and platelets were resuspended in 1 mL cold BSGC. To isolate platelets from other cellular components, the platelet suspension was centrifuged at $220g$ for 6 min at 4 °C and PR suspension was transferred to a clean Eppendorf tube. Platelets were pelleted at $1613g$ for 10 min at 4 °C and supernatant discarded. Platelets were then resuspended to appropriate volume in BSGC for immediate injection. To confirm that platelets had not become activated during the isolation procedure, a small aliquot was removed from the final suspension to be tested. Only after the addition of thrombin did the platelets clump and the previously cloudy suspension become clear. Animals received a 100-µl i.v. injection that contained platelets concentrated from 3 or 6 mL of whole murine blood. Only those vials that showed no evidence of coagulation were used for platelet isolation.

Analysis of coagulation using confocal microscopy

To enable analysis of coagulation in vivo, confocal microscopy was performed using a previously developed technique [17]. B16F10-LacZ cells were labeled in vitro using 5-chloromethylfluorescein diacetate, Cell Tracker Green (CMFDA, Molecular Probes, Burlington, Ontario, Canada), according to the manufacturer's instructions. Ten minutes before cell injection, animals received intravenous injection of 0.12 mg AlexaFluor647-conjugated fibrinogen (Molecular Probes) in 80 µl sodium bicarbonate, pH 8.3. Four hours following cell injection, animals were euthanized by an intraperitoneal injection of xylazine/ketamine (5.2 mg ketamine and 0.26 mg xylazine per 20 g body mass). The lung was cleared of blood by gravity perfusion of HBSS through the right ventricle of the heart. "Flow through" perfusate left the body via a puncture made in the left atrium. Lungs were perfused for 2 min, excised and frozen at −80 °C to allow for later analysis by confocal microscopy. To visualize, lungs were thawed in cold HBSS prior to transfer to 0.1 % paraphenylenediamine in HBSS for 10 min. Lungs were assessed using a Zeiss LSM 410 confocal microscope and Carl Zeiss LSM 3.99 software. The presence of tumor cells was determined using green fluorescence and the focal plane containing the largest volume of tumor cells was identified. At that same focal plane, the lung then was scanned for red fluorescence to identify thrombi. The green and red fluorescence were quantified in pixels by a blinded observer using ImageJ [32], and the ratio of thrombus to tumor cell area was determined. To ensure that visualized red fluorescence was due to thrombus formation and not accumulation of fluorescent fibrinogen that was not cleared, potentially due to vessel blockage by tumor cells, inert plastic

microspheres (20 μm, Polysciences, Pennsylvania) were injected. Use of these microspheres in platelet-restoration experiments allowed examination of lung tissue for non-specific thrombus formation following platelet injection.

Histology

Spleens were collected and weighed; long bones were stripped of muscle tissue prior to fixation of tissues in 10 % buffered formalin. Bones were decalcified in Cal-Ex II (Fischer Scientific, New Jersey) solution prior to H&E staining of 3-μm sections. Megakaryocyte quantification was carried out by a trained observer under pathologist guidance.

Statistical analysis

The Student's unpaired t test and one-way ANOVA with a Tukey's multiple comparisons post-test were used to compare between animal groups. The Pearson's rank correlation was used to determine relationships between various variables. All statistics were calculated using GraphPad Prism 4. A two-sided $P < 0.05$ was considered statistically significant.

Results

To evaluate the effect of a primary tumor on early steps in the development of metastases, we quantified metastases using a modified model of experimental metastasis. Animals first received an intradermal (i.d.) injection of B16F10 cells (primary tumor group) or cell vehicle (tumor-naïve group). After 16 days, all animals received a secondary injection of B16F10-LacZ cells via the lateral tail vein to target cells directly to the lung. Primary tumors were 533.5 ± 33.2 mm^3 at the time of secondary injection. We found that the presence of a primary tumor significantly inhibited experimental lung metastasis, as 6 days following secondary injection, there were fewer X-gal positive lung surface metastases in primary tumor-bearing mice as compared to tumor-naïve animals (Fig. 1a). Very few lung metastases were not positive for X-gal (three metastases in all mice examined), and these tumors were significantly larger than the other metastases visualized. It was assumed that these rare metastases arose from seeding by the primary tumor and were not included in subsequent quantification. X-gal positive metastases that did form in the primary tumor group were significantly smaller than those in the tumor-naïve group (Fig. 1b), indicating that the primary tumor is not only impeding survival of arrested cells but also the growth of cells that do persist.

Previous work in our and other laboratories [17, 20, 21] has shown that efficient metastasis of B16F10 cells is dependent on thrombus formation at the cell surface following arrest in the lung microvasculature. Therefore, we evaluated the ability
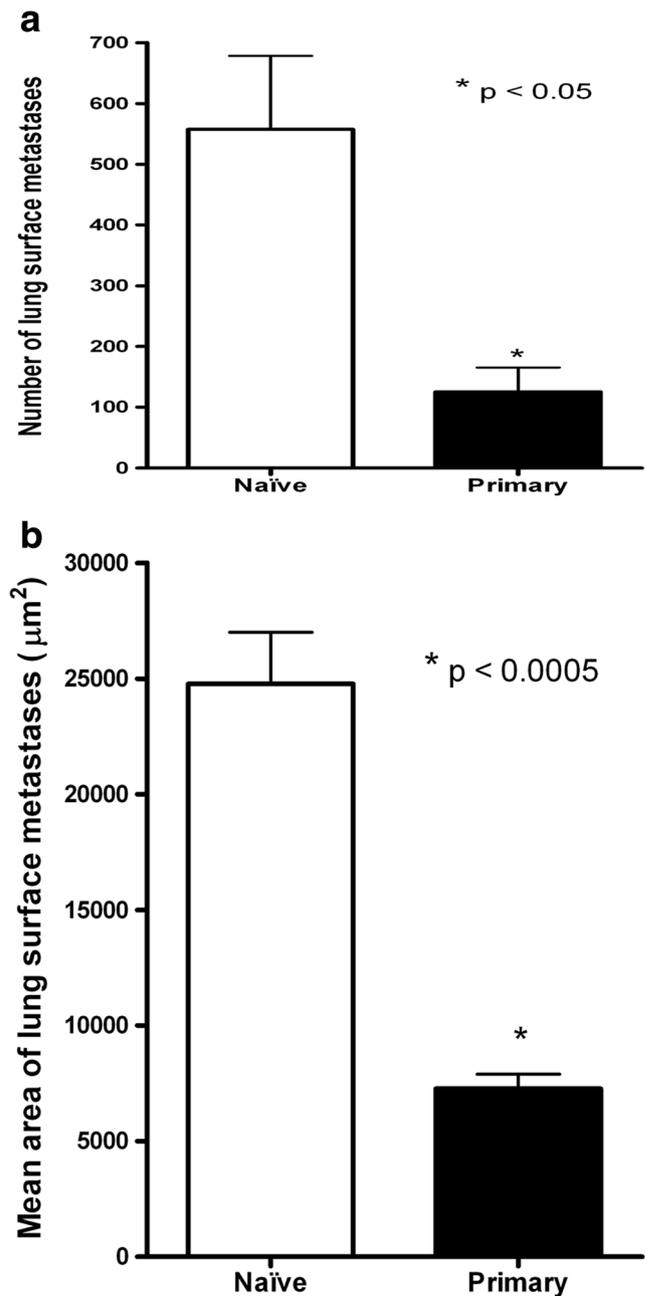
Fig. 1 The presence of an intradermal B16F10 primary tumor significantly reduced lung metastasis from a secondary i.v. injection of B16F10-LacZ cells. **a** Animals that received an i.d. injection of B16F10 cells had fewer lung metastases than did animals that received a sham i.d. injection ($n = 10$–12/group; t test $p < 0.05$). **b** Lung metastases that developed in tumor-bearing mice were significantly smaller than those in tumor-naïve animals ($n = 4$/group, randomly chosen from animals in **a**; t test $p < 0.005$). Columns, mean; bars, SE

of B16F10-LacZ cells to stimulate thrombus formation following arrest in the lung of tumor-bearing and tumor-naïve animals. Using a previously developed confocal microscopy technique [17], we found that the presence of a primary tumor significantly reduced the size of thrombi that formed 4 h after secondary cell injection as compared to tumor-naïve animals

(pictured in Fig. 2a, b, quantified in Fig. 2c). As previously reported, thrombus formation as detected by this approach was associated with subsequent formation of metastatic foci [17].

To determine the mechanism by which the presence of a primary tumor inhibited thrombus formation around i.v. injected cells, the number of circulating platelets was quantified in tumor-naïve and tumor-bearing animals. Sixteen days following primary injection, blood was pulled via cardiac puncture for analysis. It was found that primary tumor-bearing mice had significantly fewer circulating platelets than tumor-naïve animals had (Fig. 3a). Primary tumor-bearing mice were also found to have significantly enlarged spleens upon sacrifice at day 16 (Fig. 3b), and spleen size significantly correlated positively with primary tumor weight (Fig. 3c) and negatively with platelet number (Fig. 3d). Tumor weight showed a trend toward a negative correlation with the number of circulating platelets (Fig. 3e), but this did not reach statistical significance.

Histological analysis of spleens from tumor-bearing and tumor-naïve animals was performed to further assess the interplay between the primary tumor and the spleen. Normal spleen histology was observed in tumor-naïve animals (Fig. 4a, b), but it was found that the spleens isolated from tumor-bearing animals with enlarged spleens showed extensive extramedullary hematopoiesis, with tri-lineage precursors throughout the red pulp, distorting the splenic architecture and decreasing white pulp presence (Fig. 4c, d). In particular, there was an abundance of megakaryocytes and their precursors (Fig. 4d vs. b). The observed splenomegaly (Fig. 3b) was thus at least in part due to marked extramedullary hematopoiesis and may have been secondary to platelet consumption in tumor-bearing animals.

To further investigate the effect of the primary tumor on platelet manufacture, long bones of primary tumor-bearing and tumor-naïve animals were removed and the number of megakaryocytes was quantified in histologic slides. Contrary to the spleen histology, there was no effect of the primary tumor on the number of megakaryocytes in the long bones (data not shown), indicating that the tumor-stimulated platelet manufacture is in the spleen alone, as is common during murine stress [33].
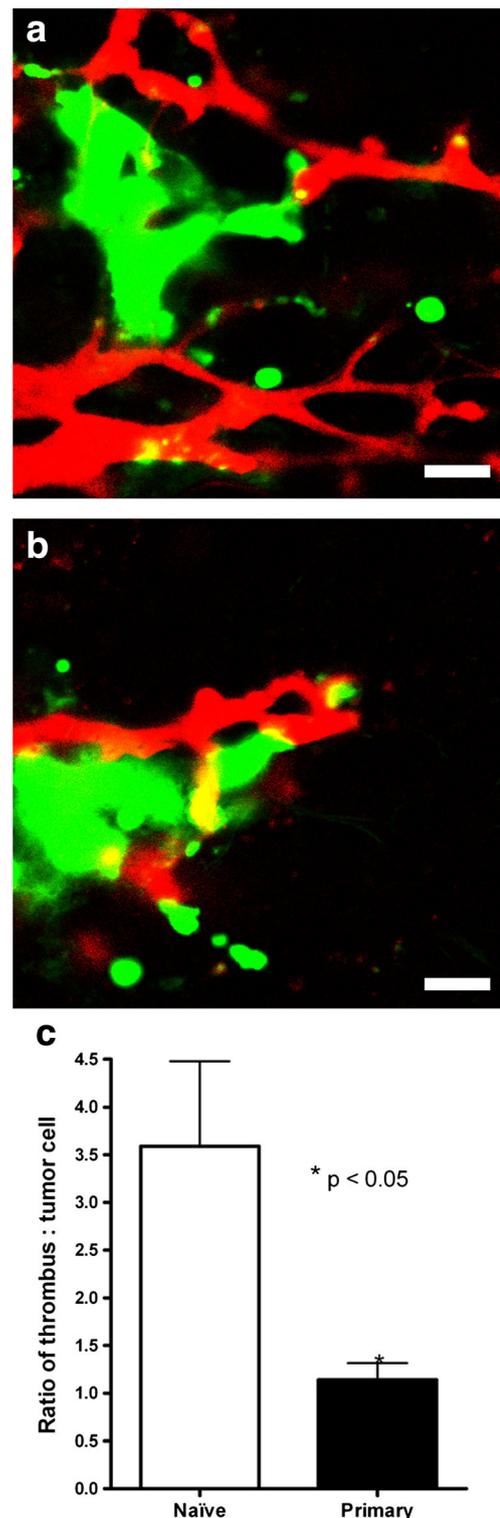
To determine if reduction in platelet number was functionally responsible for the decrease in lung metastasis, we strove to re-establish a normal platelet count in tumor-bearing mice. To this end, we isolated platelets from donor mice and injected them into tumor-bearing animals 16 days following primary tumor introduction.
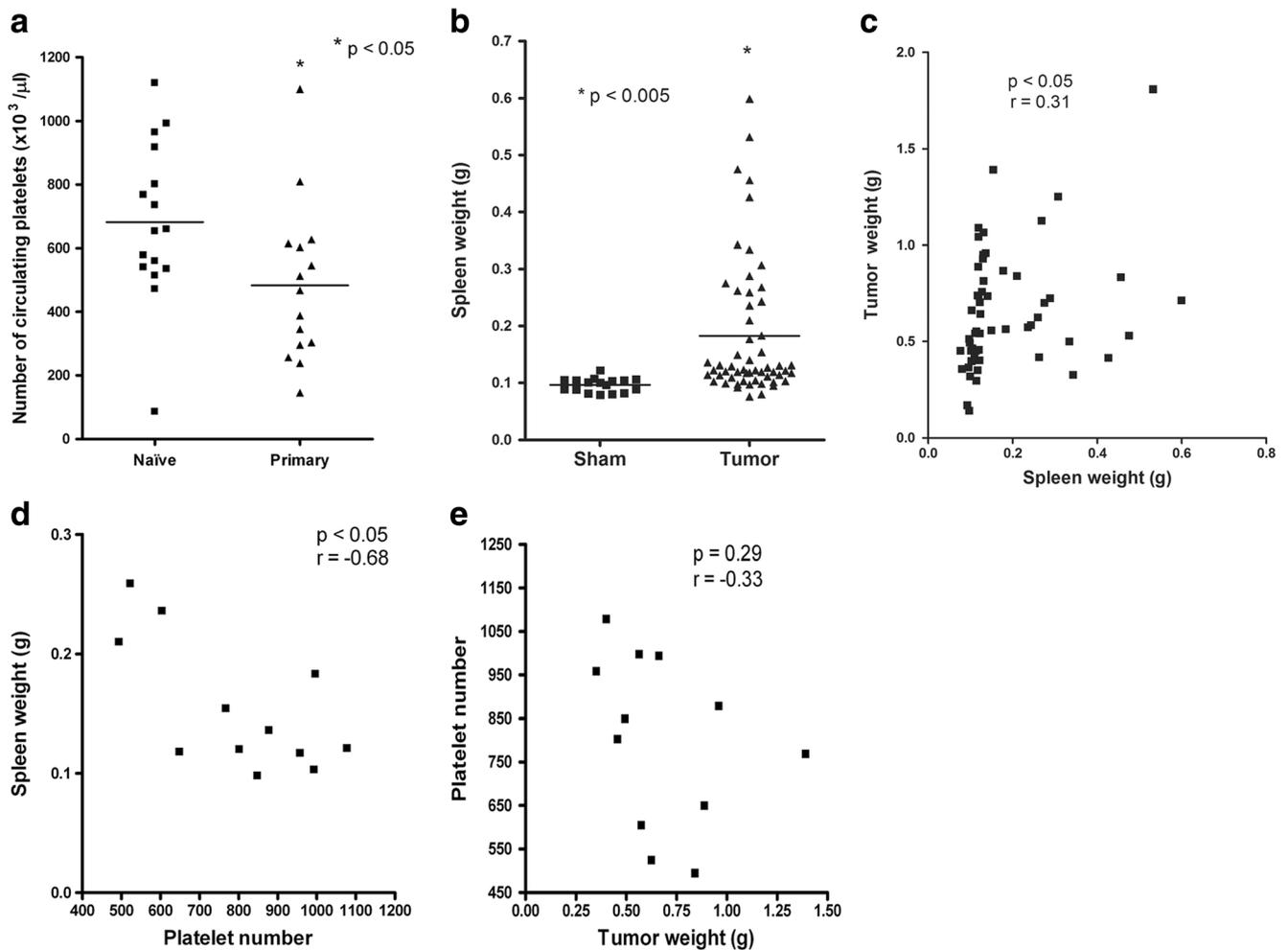
Fig. 3 Interaction between a B16F10 primary tumor and platelet turnover. **a** Quantification of circulating platelets in tumor-naïve and tumor-bearing animals. Animals with a B16F10 primary tumor had significantly fewer platelets 16 days following i.d. injection ($n = 15$–16/group, t test $p < 0.05$). **b** Tumor-bearing mice were found to have significantly enlarged spleens as compared to tumor-naïve animals ($n = 17$–56/group, t test $p < 0.005$). Additionally, spleen weight correlated with both **c** tumor size ($n = 56$, Pearson's $p < 0.05$, $r = 0.31$) and **d** platelet count ($n = 12$, Pearson's $p < 0.05$, $r = -0.68$). **e** Correlation between tumor size and platelet count did not reach significance ($n = 12$, Pearson's $p = 0.29$, $r = -0.33$)

We concentrated platelets from 3 or 6 mL of blood prior to injection and found that platelets isolated from 6 mL of mouse blood was required to fully restore the number of circulating platelets in tumor-bearing animals (Fig. 5a). We next wanted to determine if this platelet injection allowed functional thrombus formation in response to secondary cell injection. Intravenous injection of AlexaFluor647-conjugated fibrinogen prior to injection of unlabeled platelets or vehicle and CMFDA-labeled tumor cells allowed visualization of all thrombi formed in response to B16F10-LacZ tumor cells. Using confocal microscopy, we evaluated thrombus formation in tumor-naïve and tumor-bearing mice following platelet vehicle injection and tumor-bearing mice after platelet injection. Injection of platelets isolated from 6 mL of blood was capable of restoring thrombus formation in primary tumor-bearing mice to levels equivalent to tumor-naïve

animals (Fig. 5b–e). To confirm that visualized thrombi were specific to tumor cell interaction and did not arise from injection of isolated platelets, a subset of tumor-naïve animals received i.v. injection of fluorescent fibrinogen prior to injection of isolated platelets. These animals did not receive B16F10-LacZ cells; rather, they received an i.v. injection of 20-μm inert fluorescent microspheres. Arrest of these spheres did not result in thrombus formation or spontaneous fluorescent fibrinogen accumulation (Fig. 5f). This indicates that the thrombi observed following tumor cell injection are due to interaction between B16F10-LacZ cells and circulating coagulation factors.

Given that injection of platelets restored functional coagulation at the metastatic cell surface, we quantified lung metastasis formation in mice following platelet injection. Sixteen days after mice received a primary tumor or sham injection, animals received an i.v. injection of platelets or vehicle 5 min

Fig. 4 Histological analysis of splenic tissue isolated from tumor-naïve (**a**, **b**) and tumor-bearing (**c**, **d**) animals. Normal splenic structure is seen in tumor-naïve animals, with distinct red (*R*) and white pulp (*W*). Hypercellularity is seen in the red pulp of spleens isolated from tumor-bearing animals, with reduction of white pulp. Higher power magnification shows normal red pulp in tumor-naïve spleen (**b**), vs. marked tri-lineage extramedullary hematopoiesis, with a particular abundance of megakaryocytic precursors (*arrows*) in tumor-bearing animals (**d**)
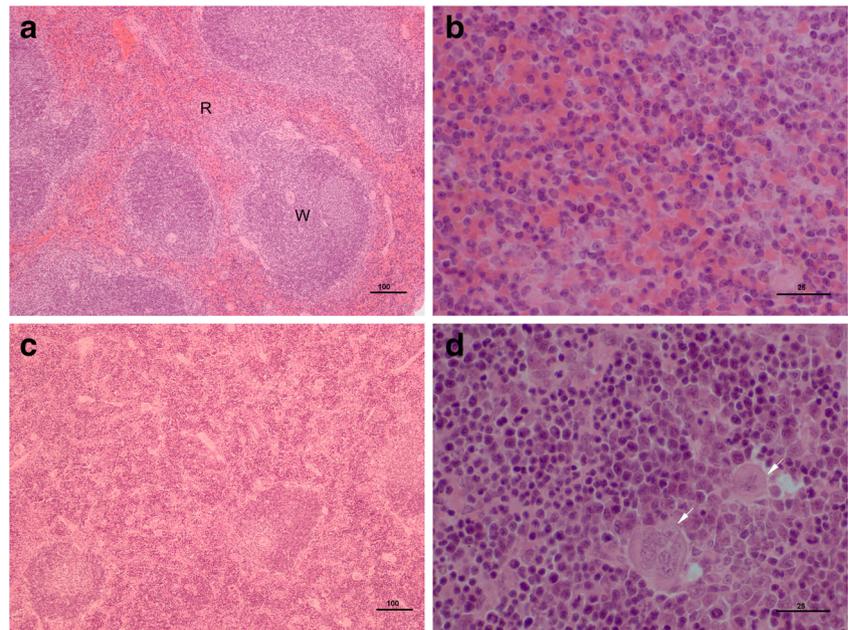
prior to i.v. injection of B16F10-LacZ cells. Six days following secondary cell injection, the number of lung surface metastases was quantified.

Tumor-naïve mice that received the platelet vehicle (Naïve Vehicle) were found to have fewer metastases as compared to un-injected, tumor-naïve mice (Naïve; Fig. 6), potentially due to the presence of the anti-coagulant EDTA in the platelet vehicle. Importantly, tumor-bearing mice that received platelets 5 min prior to i.v. injection of B16F10-LacZ cells (Primary + 6 mL Platelets) showed more lung metastases than did tumor-naïve animals that received platelet vehicle (Naïve Vehicle) and showed equivalent metastasis to un-injected tumor-naïve mice (Naïve). These results demonstrate that re-establishment of platelet number was capable of restoring lung metastasis of B16F10-LacZ cells and was able to counteract the effect of the presence of a B16F10 primary tumor (Fig. 6).

Discussion

In this study, we established that the presence of a B16F10 primary tumor was capable of significantly inhibiting the number and size of lung metastases arising from secondarily injected B16F10-LacZ cells. This inhibition of metastasis was found to be due to primary tumor-induced coagulopathy, as indicated by the reduced circulating platelet number, resulting in insufficient thrombus formation in the lung following metastatic cell injection. Restoration of circulating platelet number, through injection of platelets isolated from donor mice, re-established thrombus formation in primary tumor bearing mice and allowed equivalent metastasis formation in both primary tumor-bearing and tumor-naïve animals.

The negative impact of a B16F10 primary tumor on secondary metastasis was somewhat surprising given that the B16 cell line has been found to stimulate pre-metastatic niche formation in the lung, liver, testis, spleen, and kidney [34]. Recruitment of bone marrow-derived cells (BMDCs) to facilitate formation of a pre-metastatic niche is thought to aid metastasis formation, as VEGFR1+ cells present in the niche increase adhesion and arrest of metastatic tumor cells. Additionally, in vitro analysis in that study found that B16 cells were increasingly mobile in response to VEGFR1+ cells. It is possible that B16F10 cells do not stimulate formation of the pre-metastatic niche as seen with the B16 cells used by Kaplan et al. [34] or that the reduction in platelet number in primary tumor-bearing animals is able to inhibit metastasis formation in spite of pre-metastatic niche presence. Development of concomitant tumor resistance has been found to occur via immunogenic (small tumors, immunogenic types) and non-immunogenic mechanisms (large tumors, anti-angiogenic, or anti-mitotic mechanisms) [10, 35, 36], but the potential for a primary tumor to both inhibit and promote metastasis through concomitant tumor resistance and pre-metastatic niche formation requires further investigation. Importantly, in this study, animals received the second injection of tumor cells when the primary tumor was relatively small ($\sim$530 mm^3) such that the previously identified anti-angiogenic and anti-mitotic mechanisms of concomitant tumor resistance found to occur after primary tumors reached 1000 mm^3 [14] should not yet be involved. Additionally, immunogenic control is not thought to be responsible for the suppression of B16F10 metastases seen here, as B16 cells were derived from a spontaneously formed tumor and are poorly immunogenic [15]. Direct analysis of tumor immunity

Fig. 5 (caption described at left)

in a B16 model found that it was induction of CD4+ CD25+
regulatory T cells that prevented the development of concomi-
tant tumor immunity in C57Bl/6 mice [15].

It is well established that platelets play an integral role in
metastatic establishment [37–39]. Following arrest in the vas-
culature, some tumor cell types have been shown to stimulate
thrombus formation at their cell surface [17, 19, 21]. The
interaction between tumor cells and thrombi provides valuable
adhesion contacts [40], growth and survival factors, and pro-
tection from host immune surveillance [19, 38]. In pre-clinical
studies, treatment of animals with an anti-coagulant such as
heparin [17] or hirudin [20] prior to metastatic cell injection
results in significant reduction in pulmonary metastasis [41].
Previous work in our laboratory also found that inhibition of
serine-protease activity in vivo stabilized tumor cell-
associated thrombi and increased B16F10 metastasis forma-
tion [17]. Activated platelets were found to increase invasive-
ness of human ovarian cancer cells [28], and tumor cells that
are able to stimulate clot formation are more likely to be
retained in the pulmonary vasculature, as they are more likely
to form stable adhesive contacts and spread along the inside of
the pulmonary vasculature [18]. It also has been reported that
transgenic animals expressing a mutant form of
thrombomodulin with decreased thrombin-binding affinity
(thereby allowing increased local thrombin activity) were
found to have increased experimental and spontaneous metas-
tasis of TF-expressing tumor cells. This increase was found to
be due to a significant increase in tumor cell survival in the
lung [42]. Induction of thrombocytopenia through injection of
bacterial lipopolysaccharide or neuraminidase significantly
decreases lung metastasis of both strongly and weakly immu-
nogenic tumor types [43]. Interestingly, injection of platelets
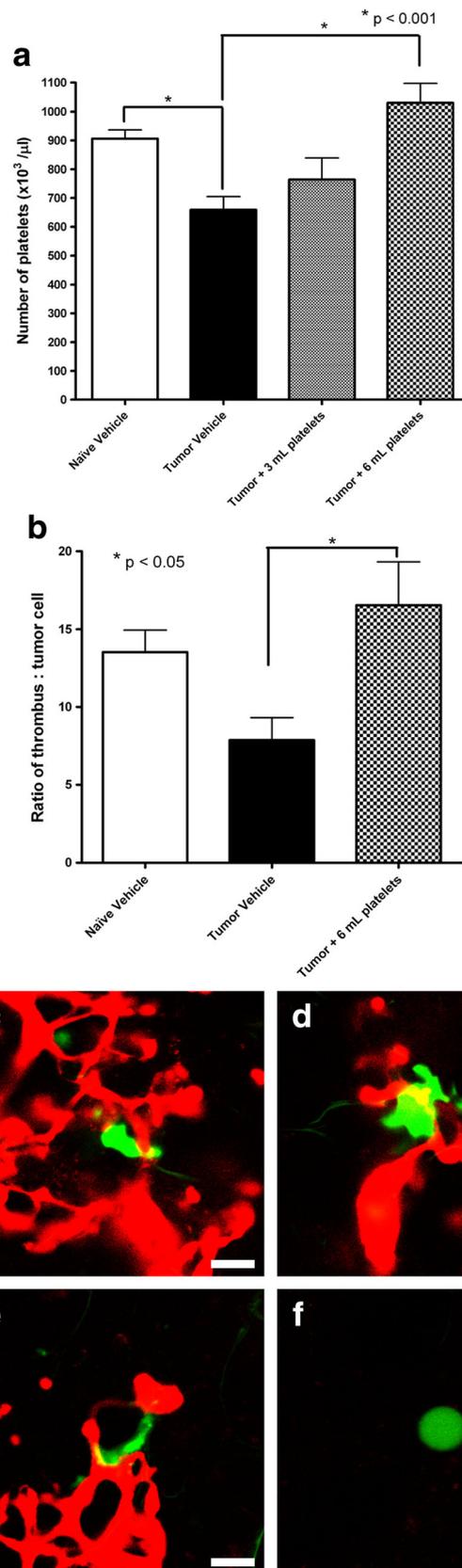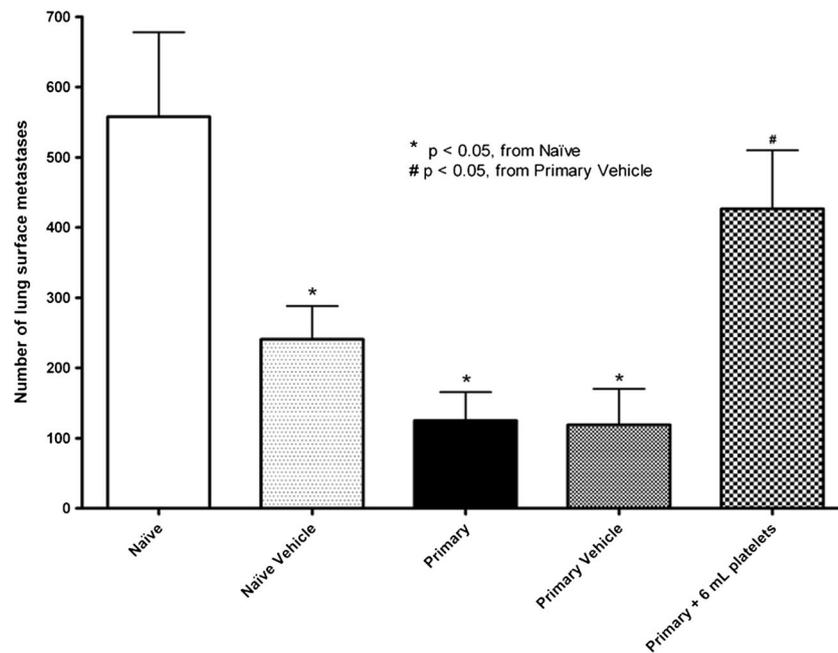
Fig. 6 Reconstitution of platelet number in tumor-bearing animals re-established lung metastasis formation. Tumor-naïve animals received an i.v. injection of platelet vehicle and tumor-bearing animals received an i.v. injection of platelet vehicle or isolated platelets prior to i.v. B16F10-LacZ cell injection ($n = 12$/group). Platelet vehicle injection into tumor-naïve animals reduced metastasis number as compared to control (un-injected naïve and primary data are historical controls from Fig. 1a) (ANOVA, Tukey's post-test, $p < 0.05$). Vehicle injection into tumor-bearing mice did not further reduce metastasis from that seen previously in tumor-bearing animals ($p > 0.05$). Platelet injection into tumor-bearing mice showed an increase in lung metastasis as compared to vehicle-injected tumor-bearing animals ($p < 0.05$) and restored lung metastasis number to that seen in tumor-naïve animals ($p > 0.05$). Columns, mean; bars, SE

into thrombocytopenic animals prior to i.v cell injection did not restore metastasis number, potentially due to insufficient platelet injection, as evidence for platelet number rescue was not presented [43]. The direct role of platelets in establishment of metastases has been investigated in B16 and fibrosarcoma models with conflicting results. The positive correlation between platelet aggregation and metastatic ability found in the B16F10 cell line did not hold when individual B16F10 clones were generated and tested [44]. Similar clonal investigation with the PAK 17 fibrosarcoma cell line showed that highly metastatic clones require platelet interaction for successful metastasis [45]. This disparity could be due to differences in analysis of platelet aggregating ability [45] but could indicate that the most aggressive B16F10 clones are capable of metastasis regardless of platelet interaction, due to other malignant characteristics. For example, those clones that exhibit high metastatic ability without extensive platelet aggregation activity may form more extensive tumor cell-tumor cell associations allowing for similar protection from immune surveillance for the central cells as is provided by thrombus formation [24]. Alternatively, these cells may indirectly stimulate platelet aggregation in vivo, which would not be readily detectable in vitro. In general, these two studies identified that high platelet aggregating ability is not sufficient for metastasis of non-metastatic cells [44] and indicate that tumor cell-thrombus association is an important determinant in metastatic potential [45].

Interestingly, the splenomegaly identified in tumor-bearing animals was associated with tri-lineage extramedullary hematopoiesis, with a preponderance of megakaryocytic precursors. A similar increase in hematopoiesis was not found in the bone marrow of tumor-bearing mice, which is in accordance with normal murine physiologic response. During stress, the majority of (reactive) hematopoiesis is performed in the murine spleen [33]. Despite the increase in platelet manufacture in the spleen, the number of circulating platelets was significantly decreased in tumor-bearing mice, indicating that the spleen was unable to replenish the platelets being lost.

Several possibilities exist for the cause of the platelet consumption and resulting thrombocytopenia in this case. B16F10 murine melanoma cells express TF on their cell surface [26, 46]; therefore, the cells within the tumor may activate circulating platelets resulting in thrombus formation at the primary tumor site. B16F10 primary tumors tend be hemorrhagic, with a necrotic core that is void of much secondary structure, and can lead to extensive bleeding with even minor trauma (unpublished observation). In addition, and perhaps most importantly, the presence of a B16F10 primary tumor may stimulate disseminated intravascular coagulation (DIC). DIC in cancer is characterized by activation of the coagulation cascade in the defective tumor vasculature or by pro-coagulant activity on tumor cells, or their membrane components, and is the most common cause of thrombocytopenia in cancer

patients [38, 47]. Local fibrinogen and platelet consumption then lead to systemic deficiencies and increased clotting time, and indeed, similar systemic coagulopathy may be present in primary tumor-bearing animals. Although human patients may be somewhat less susceptible to tumor-associated thrombocytopenia (thrombocytosis is the most common blood abnormality in cancer patients [38, 39]), mice are known to compensate poorly for blood or platelet loss and easily develop anemia or thrombocytopenia following a minor insult [33]. Interestingly, B16F10 cells have been found to generate large numbers of microvesicles (MVs) in vitro; isolation and injection of these MVs prior to i.v. injection of B16F10 cells has been linked to increased metastasis [48]. Given the cell surface expression of TF on B16F10 cells [26], it would be anticipated that these MVs would also contain TF, which could confer procoagulant activity (depending on how it was displayed and the presence of other factors within the MV). Therefore, it is possible that injection of MV 2 h prior to injection of B16F10 cells [48] could result in an increase in tumor cell-associated thrombus formation, leading to an increase in metastasis. In the presence of an ongoing release of TF-containing MV from a B16F10 primary tumor, it would be anticipated that rather than a pro-metastatic effect of the MV, there would be sustained activation of the coagulation cascade leading to platelet exhaustion and/or depletion, as was seen here. Therefore, the release of MV from the B16F10 primary tumor may be partially responsible for the significant reduction in platelet numbers.

The integral role of coagulation in metastasis formation is further indicated by the effect of anti-coagulant therapy in cancer patients. Preliminary clinical trials have shown a significant increase in overall survival of patients randomized to receive low molecular weight heparin (LMWH) versus placebo [49]. Interestingly, long-term exposure to LMWH in patients with cancer-related thrombosis only increased survival of those patients who did not have metastatic disease at the time of study enrollment [49]. Additionally, large cohort analysis of overall probability of death in those patients diagnosed with cancer as compared to those diagnosed with cancer and thromboembolism found that approximately 20 % of patients with cancer alone and 90 % of patients with a combined diagnosis succumbed to their disease within 6 months. It has been indicated that these deaths could be attributed to three possible scenarios: (1) fatal recurrent pulmonary thromboembolism; (2) identification of a coagulation disorder may simply be a surrogate marker for more aggressive malignancy; (3) systemic aberrations in the coagulation pathway may result in a more permissive tumor cell-host interaction giving rise to extensive tumor growth resulting in the early death of the patient [49]. Further, review of clinical data to evaluate anti-tumoral effects by LMWH suggests that LMWHs may improve patient survival through both prevention of venous thromboembolism and specific antitumoral effects, but these findings are mixed and further investigation on more homogenous patient populations is required to identify those groups who would benefit from targeted LMWH therapy [50, 51]. For example, as a note of caution, a recent report on the FRAGMATIC trial in lung cancer patients concluded that LMWH did not improve overall survival in this cohort of patients [52]. Given these data, further analysis of modulation of the systemic coagulation pathway in cancer patients as a means to prevent metastasis establishment and premature death is warranted.

The development of metastases occurs in the midst of a complex interaction between a primary tumor and the host—the full extent of which remains unknown. There is the potential for a primary tumor to promote metastatic progression through stimulation of pre-metastatic niche formation, as well as to restrict metastasis through concomitant tumor resistance. In this study, we identified a form of concomitant tumor resistance known as athrepsia, which was in this case due to primary tumor-induced thrombocytopenia and the resulting reduction in tumor-thrombus formation, with inhibition of metastasis. Full understanding of the interplay between a primary tumor, the host and forming metastases will be essential to the development of strategies to inhibit metastatic progression, either before or after the surgical resection of the primary tumor.

References

1. Chambers AF, Groom AC, MacDonald IC (2002) Dissemination and growth of cancer cells in metastatic sites. Nat Rev Cancer 2(8): 563–572

2. Labelle M, Hynes RO (2012) The initial hours of metastasis: the importance of cooperative host-tumor cell interactions during hematogenous dissemination. Cancer Discov 2(12):1091–1099

3. Lorusso G, Ruegg C (2008) The tumor microenvironment and its contribution to tumor evolution toward metastasis. Histochem Cell Biol 130(6):1091–1103

4. Clark WH Jr, Elder DE, Guerry D, Braitman LE, Trock BJ, Schultz D, Synnestvedt M, Halpern AC (1989) Model predicting survival in stage I melanoma based on tumor progression. J Natl Cancer Inst 81(24):1893–1904

5. Demicheli R, Retsky MW, Hrushesky WJ, Baum M, Gukas ID (2008) The effects of surgery on tumor growth: a century of investigations. Ann Oncol 19(11):1821–1828

6. Prehn RT (1991) The inhibition of tumor growth by tumor mass. Cancer Res 51(1):2–4

7. Gorelik E (1983) Concomitant tumor immunity and the resistance to a second tumor challenge. Adv Cancer Res 39:71–120

8. Chiarella P, Bruzzo J, Meiss RP, Ruggiero RA (2012) Concomitant tumor resistance. Cancer Lett 324(2):133–141

9. Galmarini CM, Tredan O, Galmarini FC (2014) Concomitant resistance and early-breast cancer: should we change treatment strategies? Cancer Metastasis Rev 33(1):271–283

10. O'Reilly MS, Holmgren L, Shing Y, Chen C, Rosenthal RA, Moses M, Lane WS, Cao Y, Sage EH, Folkman J (1994) Angiostatin: a novel angiogenesis inhibitor that mediates the suppression of metastases by a Lewis lung carcinoma. Cell 79(2):315–328

11. Holmgren L, O'Reilly MS, Folkman J (1995) Dormancy of micrometastases: balanced proliferation and apoptosis in the presence of angiogenesis suppression. Nat Med 1(2):149–153

12. Folkman J (1995) Angiogenesis inhibitors generated by tumors. Mol Med 1(2):120–122

13. O'Reilly MS, Holmgren L, Chen C, Folkman J (1996) Angiostatin induces and sustains dormancy of human primary tumors in mice. Nat Med 2(6):689–692

14. Franco M, Bustuoabad OD, Di Gianni PD, Meiss RP, Vanzulli S, Buggiano V, Pasqualini CD, Ruggiero RA (2000) Two different types of concomitant resistance induced by murine tumors: morphological aspects and intrinsic mechanisms. Oncol Rep 7(5): 1053–1063

15. Turk MJ, Guevara-Patino JA, Rizzuto GA, Engelhorn ME, Sakaguchi S, Houghton AN (2004) Concomitant tumor immunity to a poorly immunogenic melanoma is prevented by regulatory T cells. J Exp Med 200(6):771–782

16. Falanga A, Panova-Noeva M, Russo L (2009) Procoagulant mechanisms in tumour cells. Best Pract Res Clin Haematol 22(1):49–60

17. Kirstein JM, Graham KC, Mackenzie LT, Johnston DE, Martin LJ, Tuck AB, MacDonald IC, Chambers AF (2009) Effect of anti-fibrinolytic therapy on experimental melanoma metastasis. Clin Exp Metastasis 26(2):121–131

18. Im JH, Fu W, Wang H, Bhatia SK, Hammer DA, Kowalska MA, Muschel RJ (2004) Coagulation facilitates tumor cell spreading in the pulmonary vasculature during early metastatic colony formation. Cancer Res 64(23):8613–8619

19. Palumbo JS, Talmage KE, Massari JV, La Jeunesse CM, Flick MJ, Kombrinck KW, Jirouskova M, Degen JL (2005) Platelets and fibrin(ogen) increase metastatic potential by impeding natural killer cell-mediated elimination of tumor cells. Blood 105(1):178–185

20. Esumi N, Fan D, Fidler IJ (1991) Inhibition of murine melanoma experimental metastasis by recombinant desulfatohirudin, a highly specific thrombin inhibitor. Cancer Res 51(17):4549–4556

21. Palumbo JS, Kombrinck KW, Drew AF, Grimes TS, Kiser JH, Degen JL, Bugge TH (2000) Fibrinogen is an important determinant of the metastatic potential of circulating tumor cells. Blood 96(10):3302–3309

22. Palumbo JS, Potter JM, Kaplan LS, Talmage K, Jackson DG, Degen JL (2002) Spontaneous hematogenous and lymphatic metastasis, but not primary tumor growth or angiogenesis, is diminished in fibrinogen-deficient mice. Cancer Res 62(23):6966–6972

23. Palumbo JS, Talmage KE, Liu H, La Jeunesse CM, Witte DP, Degen JL (2003) Plasminogen supports tumor growth through a fibrinogen-dependent mechanism linked to vascular patency. Blood 102(8):2819–2827

24. Palumbo JS, Talmage KE, Massari JV, La Jeunesse CM, Flick MJ, Kombrinck KW, Hu Z, Barney KA, Degen JL (2007) Tumor cell-associated tissue factor and circulating hemostatic factors cooperate to increase metastatic potential through natural killer cell-dependent and-independent mechanisms. Blood 110(1):133–141

25. Palumbo JS, Barney KA, Blevins EA, Shaw MA, Mishra A, Flick MJ, Kombrinck KW, Talmage KE, Souri M, Ichinose A et al (2008) Factor XIII transglutaminase supports hematogenous tumor cell metastasis through a mechanism dependent on natural killer cell function. J Thromb Haemost 6(5):812–819

26. Kirszberg C, Lima LG, Da Silva de Oliveira A, Pickering W, Gray E, Barrowcliffe TW, Rumjanek VM, Monteiro RQ (2009) Simultaneous tissue factor expression and phosphatidylserine exposure account for the highly procoagulant pattern of melanoma cell lines. Melanoma Res 19(5):301–308

27. Gay LJ, Felding-Habermann B (2011) Contribution of platelets to tumour metastasis. Nat Rev Cancer 11(2):123–134

28. Holmes CE, Levis JE, Ornstein DL (2009) Activated platelets enhance ovarian cancer cell invasion in a cellular model of metastasis. Clin Exp Metastasis 26(7):653–661

29. Orellana R, Kato S, Erices R, Bravo ML, Gonzalez P, Oliva B, Cubillos S, Valdivia A, Ibanez C, Branes J et al (2015) Platelets enhance tissue factor protein and metastasis initiating cell markers, and act as chemoattractants increasing the migration of ovarian cancer cells. BMC Cancer 15:290

30. Schmitt A, Guichard J, Masse JM, Debili N, Cramer EM (2001) Of mice and men: comparison of the ultrastructure of megakaryocytes and platelets. Exp Hematol 29(11):1295–1302

31. Musaji A, Vanhoorelbeke K, Deckmyn H, Coutelier JP (2004) New model of transient strain-dependent autoimmune thrombocytopenia in mice immunized with rat platelets. Exp Hematol 32(1):87–94

32. Schneider CA, Rasband WS, Eliceiri KW (2012) NIH Image to ImageJ: 25 years of image analysis. Nat Methods 9(7):671–675

33. Everds NE (2007) Hematology of the laboratory mouse. In: Fox JG, Davisson MT, Quimby FW, Barthold SW, Newcomer CE, Smith AL (eds) The mouse in biomedical research, vol 3, 2nd edn. Elsevier, Inc., Burlington, pp 133–170

34. Kaplan RN, Riba RD, Zacharoulis S, Bramley AH, Vincent L, Costa C, MacDonald DD, Jin DK, Shido K, Kerns SA et al (2005) VEGFR1-positive haematopoietic bone marrow progenitors initiate the pre-metastatic niche. Nature 438(7069):820–827

35. Franco M, Bustuoabad OD, di Gianni PD, Goldman A, Pasqualini CD, Ruggiero RA (1996) A serum-mediated mechanism for concomitant resistance shared by immunogenic and non-immunogenic murine tumours. Br J Cancer 74(2):178–186

36. Ruggiero RA, Bustuoabad OD, Bonfil RD, Meiss RP, Pasqualini CD (1985) "Concomitant immunity" in murine tumours of non-detectable immunogenicity. Br J Cancer 51(1):37–48

37. Borsig L (2008) The role of platelet activation in tumor metastasis. Expert Rev Anticancer Ther 8(8):1247–1255

38. Green DL, Karpatkin S (2009) Effect of cancer on platelets. Cancer Treat Res 148:17–30

39. Nash GF, Turner LF, Scully MF, Kakkar AK (2002) Platelets and cancer. Lancet Oncol 3(7):425–430

40. McCarty OJ, Mousa SA, Bray PF, Konstantopoulos K (2000) Immobilized platelets support human colon carcinoma cell tethering, rolling, and firm adhesion under dynamic flow conditions. Blood 96(5):1789–1797

41. Niers TM, Bruggemann LW, Klerk CP, Muller FJ, Buckle T, Reitsma PH, Richel DJ, Spek CA, Van Tellingen O, Van Noorden CJ (2009) Differential effects of anticoagulants on tumor development of mouse cancer cell lines B16, K1735 and CT26 in lung. Clin Exp Metastasis 26(3):171–178

42. Horowitz NA, Blevins EA, Miller WM, Perry AR, Talmage KE, Mullins ES, Flick MJ, Queiroz KC, Shi K, Spek CA et al (2011) Thrombomodulin is a determinant of metastasis through a mechanism linked to the thrombin binding domain but not the lectin-like domain. Blood 118(10):2889–2895

43. Kimoto M, Ando K, Koike S, Matsumoto T, Jibu T, Moriya H, Kanegasaki S (1993) Significance of platelets in an antimetastatic activity of bacterial lipopolysaccharide. Clin Exp Metastasis 11(3): 285–292

44. Kimura AK, Mehta P, Xiang JH, Lawson D, Dugger D, Kao KJ, Lee-Ambrose L (1987) The lack of correlation between experimental metastatic potential and platelet aggregating activity of B16 melanoma clones viewed in relation to tumor cell heterogeneity. Clin Exp Metastasis 5(2):125–133

45. Mahalingam M, Ugen KE, Kao KJ, Klein PA (1988) Functional role of platelets in experimental metastasis studied with cloned murine fibrosarcoma cell variants. Cancer Res 48(6):1460–1464

46. Kirszberg C, Rumjanek VM, Monteiro RQ (2005) Assembly and regulation of prothrombinase complex on B16F10 melanoma cells. Thromb Res 115(1–2):123–129

47. Kvolik S, Jukic M, Matijevic M, Marjanovic K, Glavas-Obrovac L (2010) An overview of coagulation disorders in cancer patients. Surg Oncol 19(1):e33–e46

48. Lima LG, Chammas R, Monteiro RQ, Moreira ME, Barcinski MA (2009) Tumor-derived microvesicles modulate the establishment of metastatic melanoma in a phosphatidylserine-dependent manner. Cancer Lett 283(2):168–175

49. Kakkar AK (2009) Antithrombotic therapy and survival in cancer patients. Best Pract Res Clin Haematol 22(1):147–151

50. Kakkar AK, Macbeth F (2010) Antithrombotic therapy and survival in patients with malignant disease. Br J Cancer 102(Suppl 1):S24–S29

51. Franchini M, Mannucci PM (2015) Low-molecular-weight heparins and cancer: focus on antitumoral effect. Ann Med 47(2):116–121

52. Macbeth F, Noble S, Evans J, Ahmed S, Cohen D, Hood K, Knoyle D, Linnane S, Longo M, Moore B et al (2016) Randomized phase III trial of standard therapy plus low molecular weight heparin in patients with lung cancer: FRAGMATIC trial. J Clin Oncol 34(5): 488–494